Controlled current matching in small molecule organic tandem solar cells using doped spacer layers

Rico Schueppel,[1] Ronny Timmreck,[1] Nikola Allinger,[1] Toni Mueller,[1] Mauro Furno,[1] Christian Uhrich,[2] Karl Leo,[1] and Moritz Riede[1,a)]
[1]*Institut für Angewandte Photophysik, Technische Universität Dresden, Dresden 01062, Germany*
[2]*Heliatek GmbH, Dresden, Germany*

(Received 11 August 2009; accepted 30 November 2009; published online 17 February 2010)

Current matching of the subcells is crucial to optimize the performance of tandem solar cells. Due to the thin film optics of organic solar cells, the position of the two subcells relative to the reflecting electrode becomes a very important issue. This is demonstrated for an indium tin oxide (ITO)/pin/pii/Al structure with thin intrinsic absorbing layers consisting of zinc-phthalocyanine and fullerene C_{60} and a metal-free lossless recombination contact between the subcells. By keeping the thickness of the absorbing layers constant and changing only the thickness of the inner p-doped transparent layer in 16 steps from 0 to 186 nm, the distance of the ITO-sided subcell from the reflecting electrode (Al) is systematically varied. Thus, the p-doped layer works as an optical spacer between both subcells. The influence of its thickness on the thin film optics is shown in optical simulations and confirmed with current-voltage measurements. If both subcells are separated only by the recombination contact, they are positioned in the first interference maximum of the incident light and the currents of the individual subcells nearly matches. By increasing the spacer layer thickness, the ITO-sided subcell is moved to the first interference minimum, limiting the measured short circuit current density j_{sc} of the tandem solar cell to about 1/2 of its initial value without spacer. At a spacer thickness of about 140 nm, j_{sc} recovers in the second interference maximum to nearly its original value. Within this series, an almost constant high fill factor of about 59% as well as a constant open circuit voltage of 1.06 V is observed, showing that the Ohmic losses in the spacer are negligible. The power conversion efficiency of these devices reaches nearly 4% in the first and approximately 3.6% in the second interference maximum, respectively, in an outdoor test at 1 sun. Furthermore, it is shown that for thicker absorber layers, an optimized current density cannot be reached in the first, but only in the second optical interference maximum, making the presented optical spacer an essential component for efficient organic tandem devices. © *2010 American Institute of Physics*. [doi:10.1063/1.3277051]

I. INTRODUCTION

Tandem solar cells are a promising concept to overcome the limits of a solar cell with only one band gap, that is, the Shockley-Queisser limit.[1] They can reduce the two major loss mechanisms: thermalization losses and losses via sub-band-gap transmission of photons.[2] To make use of these advantages, the three main requirements for efficient tandem solar cells are current matching of the subcells, a lossless recombination contact between the subcells, and—if possible—a complementary absorption of the subcells.

This concept is frequently used for solar cells based on inorganic semiconductors to increase the power conversion efficiency.[3] Similarly, much effort is put into realizing organic tandem solar cells because this concept can additionally tackle two of their main drawbacks:[4] (a) most used organic materials show discrete absorption features and cover only a limited range of the solar spectrum; (b) organic solar cells are dominated by excitonic effects, low charge carrier mobilities and lifetime,[5] limiting the layer thickness for light absorption. Thus, stacking complementary thin absorber materials is expected to improve the device efficiency compared to what is possible with a single heterojunction device.[6]

However, organic solar cells have typically a thickness below 300 nm and, because the sun light has to be considered as coherent on a scale of 1–2 periods of the incident light wave,[7] the optics of organic solar cells are in most cases dominated by interference effects caused by the reflecting back electrode. This becomes particularly important in the concept of pin devices, where the thin intrinsic absorbing layer—typically between 20 and 50 nm—is sandwiched between p-doped and n-doped wide-gap transport layers.[8]

Consequently, to tailor the current matching of both subcells in organic tandem solar cells, a detailed understanding of the thin film optics is required. In the present work, an indium tin oxide (ITO)/pin/pii/Al tandem solar cell structure with optically transparent p- and n-doped transport layers is used, as shown in Fig. 1. The intrinsic layers (i) consist of zinc-phthalocyanine (ZnPc) as donor and fullerene C_{60} as acceptor, a standard material combination for organic solar cells based on small molecules. The ZnPc-C_{60} combination represents the absorbing part of each subcell. Using a constant thickness of the intrinsic layers, the distance of the ITO-sided subcell from the reflecting electrode (Al) is sys-

a)Electronic mail: moritz.riede@iapp.de.

 © 2010 American Institute of Physics

Author complimentary copy. Redistribution subject to AIP license or copyright, see http://jap.aip.org/jap/copyright.jsp

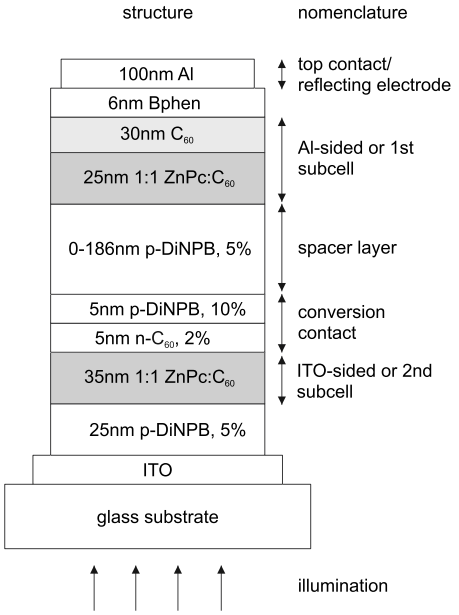

FIG. 1. Layer sequence of pin/pii tandem cell including p-doped hole transport layers (p-DiNPB), n-doped electron transport layer (n-C_{60}), intrinsic EBLs (BPhen), and absorbing layers consisting of ZnPc and C_{60} (gray). The percentages give the doping ratio by weight.

tematically varied by changing the thickness of the inner p-doped transport layer, working as a transparent optical spacer between both subcells.

Depending on the processing technology of the organic tandem solar cell, the issue of an efficient recombination contact is realized in different ways. At the recombination contact, electrons should recombine with holes without energy loss; metal clusters or thin metal layers (Au, Ag, Al), are widely used[9–15] as well as TiO_x, ZnO, or other transparent metal oxide interlayers.[16,17] Recently, it was demonstrated that highly doped transparent organic layers can be used as recombination contact with negligible energy loss.[18] In consequence, the open circuit voltage V_{oc} is a summation of the V'_{oc} of both subcells. Complementary absorption, the third requirement, is not realized in this study, because we focus on the issue of current matching. However, the presented principles are easily applicable to complementary absorber, materials in the subcells.

First, we simulate and discuss the thin film optics of these devices. The absorption profile and the simulated short circuit current density j'_{sc} of each subcell is estimated from the absorbed photon flux per subcell. Especially j'_{sc} from the ITO-sided subcell shows a strong dependence on the transparent spacer thickness. It starts at a maximum for no spacer, goes through a minimum, and nearly completely recovers in the second interference maximum. Second, the measured current-voltage characteristics of these devices and their respective variations as function of spacer thickness are presented and compared with the optical simulation. The measurements are performed on a sun simulator and under outdoor conditions to verify the indoor measurements with respect to standard reporting conditions.[19] The obtained data confirm that the optical spacer has a large impact on j_{sc} due to current matching.

The data furthermore show no influence of the spacer thickness on the series resistance of the device. Thus, the absorber layers of the subcells can be positioned relatively freely within the stack to obtain current matching. This flexibility will become essential for higher efficiencies in tandem devices using thicker absorbing layers than the ones discussed.

II. EXPERIMENTAL

The organic tandem solar cells are prepared in a multisource vacuum chamber (K.J. Lesker, UK) on a 15 $\times$ 15 cm^2 glass wafer with a prestructured ITO-coating (Thin Film Devices Ltd.). On each wafer, 4 $\times$ 4 different substrates (2.5 $\times$ 2.5 cm^2) can be prepared with each substrate consisting of four identical devices (7.34 mm^2 active device area[20]) The wafer is cleaned in a multistep wet process using acetone, ethanol, and ozone treatment. The layers are deposited by vacuum sublimation (base pressure $\leqslant 10^{-7}$ mbar) through shadow masks. Using a flexible shadow mask system during deposition, substrates can be addressed in single rows and columns. Here, this system is used to achieve a dense gradient of the spacer thickness in the device structure shown in Fig 1. Sixteen samples with a spacer layer thickness ranging from 0 to 186 nm are processed in one run under the same conditions without breaking the vacuum.

The investigated tandem structure is based on the pin-concept.[8,21] On top of the ITO a 1 nm NDP9 layer for improved ohmic contact is used, followed by a 25 nm layer of N,N′-diphenyl-N,N′-bis(4′-(N,N-bis(naphth1yl)-amino)-biphenyl-4-yl)-benzidine (DiNPB) p-doped with NDP9 (5 wt %). The absorbing layer of the ITO-sided subcell (second subcell) consists of a 35 nm ZnPc:C_{60} blend layer (1:1 by volume). The recombination contact is made of a 5 nm C_{60} layer n-doped with NDN1 (2 wt %) and a 5 nm DiNPB layer highly p-doped by NDP9 (10 wt %). The *spacer layer* consists of DiNPB doped by 5 wt % of NDP9 with varying thickness from 0 to 186 nm. The active material of the Al-sided subcell (first subcell) is again a 1:1 blend of ZnPc:C_{60} with 25 nm thickness followed by a 30 nm pristine C_{60} layer. As final organic layer, 6 nm of bathophenanthroline (BPhen) working as exciton blocking layer (EBL) is deposited. The cathode is realized depositing 100 nm Al on top of BPhen. During evaporation, the wafer is held at ambient temperature. The total thickness of the organic layers in the stack is between 131 and 317 nm.

After preparation, the devices are encapsulated using UV-curing epoxy and a cover glass in a glovebox attached to the vacuum system. A moisture getter sheet (desiccant pad) from Dynic Ltd. (China) in a cavity of the cover glass protects the organic layers. The device lifetime of such ZnPc:C_{60} tandem solar cells has been determined to be above 1500 h;[22] our measurements are performed in a fraction of this time. Thus, the devices can be considered stable during all shown measurements.

The inner p-layer is partly used for the recombination contact (5 nm highly p-doped DiNPB) connecting the two subcells and partly as hole transport layer (p-doped DiNPB) working as the optical spacer between both absorbing layers. The recombination contact is realized by doped layers with-

Author complimentary copy. Redistribution subject to AIP license or copyright, see http://jap.aip.org/jap/copyright.jsp

out using metal clusters, allowing for an almost complete summation of the open circuit voltages V'_{oc} of the subcells.[18] Instead of the commonly used p-dopant tetra-fluoro-tetracyano-quinodimethane (F4-TCNQ) and n-dopant acridine orange base (AOB), NDP9 and NDN1 are used here because of a better processability. Their performance, however, is comparable.[23,24] The basic principles of thin film optics discussed in this paper are not influenced by the choice of dopants.

DiNPB is purchased from Sensient AG (Germany) and purified twice by temperature gradient vacuum sublimation (TGVS).[25] The dopants NDP9 and NDN1 are purchased from Novaled AG (Germany). ZnPc and BPhen are delivered by ABCR GmbH (Germany) and C_{60} by the Kurchatov Institute (Russia), all being purified three times by TGVS.

Calculations of the device thin film optics are carried out using a simulation program based on the transfer matrix formalism.[26] The device structure is described as a one-dimensional assembly of homogeneous and isotropic layers with flat interfaces. The layer sequence modeled is characterized by the optical constants and the thickness of the specific materials. For thin coherent layers, the position-dependent spectral light energy flux Φ is obtained by evaluation of the component of the Poynting vector in the direction perpendicular to the interfaces between the layers.[27] For the thick incoherent substrate, Φ is directly computed from the electromagnetic field intensity. The number of absorbed photons n_{ph} per unit area, per unit time, and per unit propagation length for a given illumination spectrum is finally obtained by (1) conversion of Φ into the corresponding spectral photon flux, (2) integration of the spectral photon flux over wavelength, and (3) differentiation of the latter quantity with respect to position. The optical constants of the organic materials are extracted from reflection and transmission measurements on pristine films with different known layer thicknesses by an iterative fitting algorithm.[8,28] Additionally, these values are confirmed by an algorithm based on transmission measurements and applying Lorentz and Cauchy dispersion models.[29] The optical constants are cross-checked with ellipsometry measurements. Optical constants of Al and ITO are taken from the commercially available ETFOS database, purchased from Fluxim AG (Switzerland). For the p-DiNPB layers, n&k values of DiNPB with 5% doping and for the n-C_{60} layers, n&k values of pristine C_{60} are used.

The devices are measured with simulated sun light from a Steuernagel SC 1200 sun simulator. Its intensity is set to 100 mW/cm^2 with respect to a certified reference cell (CRC) from Fraunhofer ISE CalLab (Germany). The outdoor measurements are performed on May 8, 2008, a cloud-free day, between 11 a.m. and 1 p.m. CEST at an ambient temperature of 22 °C at location Dresden [51°01′47.5″N, 13°43′45.3″E (Ref. 30)]. The test sample and the CRC are installed in one plane on an equatorial mounting facing the sun. The normal incidence of sunlight is checked by shading and kept by a manual one-axis tracking. During the measurement time, the real sun intensity remained 1.05 ± 0.05 suns with respect to the CRC AM1.5g calibration. Values of j_{sc} discussed in this paper always refer to 100 mW/cm^2 (1.0 sun).

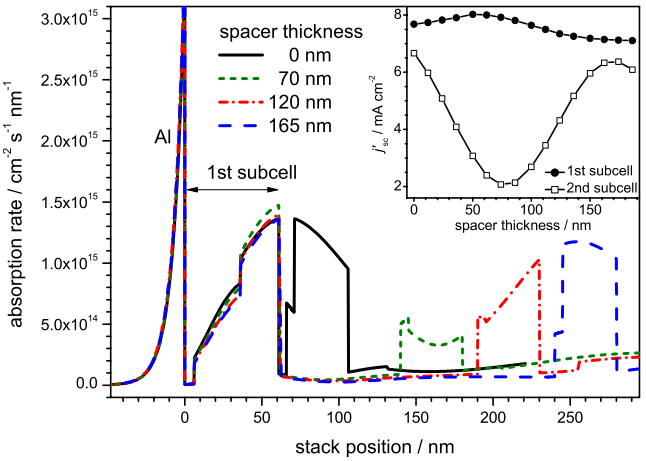

FIG. 2. (Color online) Calculated profile of the number n_{ph} of absorbed photons per unit area, time, and propagation length caused by perpendicular AM1.5g illumination of the discussed ITO/pin/pii/Al device structure. The interface of the reflecting electrode (Al) and the EBL (BPhen) is set to stack position 0 nm; the spacer layer starts at stack position 61 nm. Inset: Calculated j'_{sc} for the first subcell (30 nm C_{60}+25 nm ZnPc:C_{60}) and second subcell (35 nm ZnPc:C_{60}) assuming an IQE of unity.

III. OPTICAL SIMULATION

To achieve a detailed understanding of possible interference effects, the exciton generation profile is studied by numerical simulation. The device structure for simulations and experiments is shown in Fig. 1. Only the thickness of the spacer layer is systematically varied, and the other layers remain the same for all devices. In particular, the thickness of the absorbing layers is kept constant. Variations in the spacer layer thickness (0–186 nm) result in changes of the thin film optics of the device, which are dominated by the interference pattern forming at the reflective Al-cathode.

The calculations are carried out for AM1.5g illumination under normal incidence through the glass substrate from 350–890 nm with an integrated value of 2.1×10^{17} photons/cm^2 s. In Fig. 2, the corresponding number n_{ph} of absorbed photons per unit area, time, and propagation length is shown. The position in the stack is counted from the interface of the reflecting Al contact and BPhen. Hence, the first subcell is always located at the same position, whereas the second subcell is systematically moved further away from the Al contact with increasing spacer thickness.

Without spacer, the active layers of both subcells are located in the first maximum (black solid line). 6 nm transparent BPhen is followed by 30 nm of C_{60} that mainly absorbs below 500 nm. The increasing absorption in C_{60} with increasing distance from Al is a direct consequence of the thin film optics as the intensity rises starting from a node at the Al-cathode. The step in the absorption rate at 36 nm represents the interface between C_{60} and ZnPc:C_{60}, because ZnPc additionally absorbs in the range from 600 to 800 nm. Between 61 and 66 nm stack positions, the p-DiNPB part of the recombination contact hardly absorbs in the visible range and the absorption rate drops close to zero. The n-type part of the recombination contact consists of C_{60} and its parasitic absorption is seen as small shoulder in the absorption rate for the next 5 nm. At 71 nm the absorbing ZnPc:C_{60} layer of the

Author complimentary copy. Redistribution subject to AIP license or copyright, see http://jap.aip.org/jap/copyright.jsp

second subcell follows and the absorption rate is rising again to a similar level as in the first subcell. With increasing stack position, the absorption rate n_{ph} decreases within the ZnPc:C_{60} of the second subcell indicating the decline of the first interference maximum. Finally, from 106 nm in the stack the 25 nm p-doped DiNPB marginally absorbs in the UV below 400 nm. The increase in absorption rate indicates the second interference maximum of the shorter wavelength range, followed by parasitic absorption in the ITO.

Introducing the optical spacer, the absorbing ZnPc:C_{60} layer of the second subcell is shifted relative to the reflecting Al electrode while the first subcell remains at the same relative position. For a 70 nm thick spacer layer, the absorption rate in the second subcell is reduced to approximately 50% (green short-dashed line). The shape of the absorption rate in the range of 145–180 nm suggests a minimum in the interference system. The interference minimum does not correspond to a zero absorption rate due to the spectrally broad illumination source: the zero field strength of the interfering monochromatic waves is located at different positions within the stack. The reduced absorption in the second subcell allows for an only slightly increased absorption in the first subcell. At a spacer thickness of 120 nm, the second subcell is getting closer to the second interference maximum (red dot-dashed line), which is reached for a 165 nm spacer thickness (blue dashed line). In both latter cases the absorption in the blend part of the first subcell is as without spacer; only in the pristine C_{60} layer it is slightly reduced. This is a consequence of the increased difference in distance between the second blue and red interference maxima.

The inset of Fig. 2 shows the short circuit current densities j'_{sc} of each subcell calculated from the optical simulations. An internal quantum efficiency (IQE) of unity is assumed for the photons absorbed in the active layers. For the first subcell, j'_{sc} is obtained by adding the fluxes calculated for the ZnPc:C_{60} layer and the 30 nm of the adjacent C_{60} layer.[31] For the second subcell the calculations are based on the complete ZnPc:C_{60} layer.

The absorption and the corresponding calculated j'_{sc} of the second subcell varies strongly with the stack position, reflecting the periodic interference pattern in the device. For a spacer thickness of about 75 nm, the second subcell delivers its minimum j'_{sc}, a consequence of the thin film optics. The change between maximum and minimum j'_{sc} of the second subcell equals a factor of about 3. j'_{sc} of the first subcell reflects only slightly the reduced absorption of the second subcell. It remains nearly constant for all spacer thicknesses, indicating that the absorption in the two subcells hardly has an effect on each other in this configuration.

Thus, the simulation suggests, a spacer thickness close to 0 nm spacer thickness and at 170 nm will lead to the maximum current density (approximately 6.6 mA/cm^2) in the tandem device, with the second subcell still slightly limiting the current.

IV. EXPERIMENTAL RESULTS

Figure 3 shows the current-voltage characteristics of selected tandem devices with different spacer thicknesses that

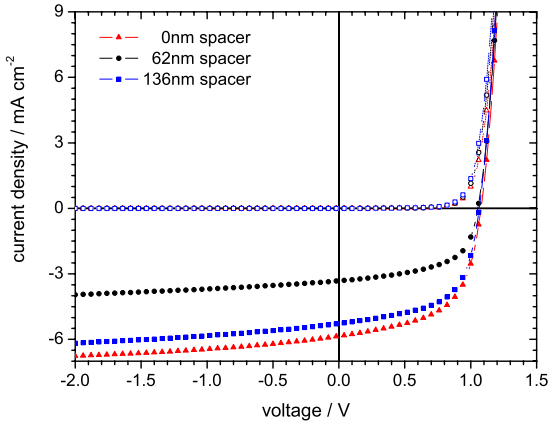

FIG. 3. (Color online) JV curves in the dark (open symbols) and under illumination (solid symbols) of ZnPc:C_{60} tandem cells with 0, 62, and 136 nm spacer layer thickness. Illumination is provided by a Steuernagel SC1200 sun simulator at 100 mW/cm^2 for a certified Si-reference cell.

demonstrate the simulated effect of the thin film optics on the device performance. In the dark the characteristics are identical. Under illumination all devices exhibit a comparable V_{oc}, fill factor FF and saturation in reverse bias. V_{oc} as well as the FF appear not to be influenced by the spacer thickness variation. The V'_{oc} of ZnPc:C_{60} single cells typically ranges around 0.55 V, slightly depending on the material quality.[25] In the tandem solar cells reported here, a V_{oc} of around 1.05–1.08 V is observed. Only the difference in j_{sc} is significant. Without spacer, both subcells are located in the first interference maximum. For 62 nm spacer, the second subcell is located close to the interference minimum, while the photocurrent with a 136 nm spacer thickness is approaching the second maximum.

In Fig. 4, j_{sc}, V_{oc}, FF as well as the power conversion efficiency η are plotted versus the spacer thickness in 15 steps from 0 to 186 nm. Any influence on the device performance due to different preparation conditions can be excluded, because all devices are processed in the same run under the same conditions.

From the optical simulations, a periodic variation of j_{sc}

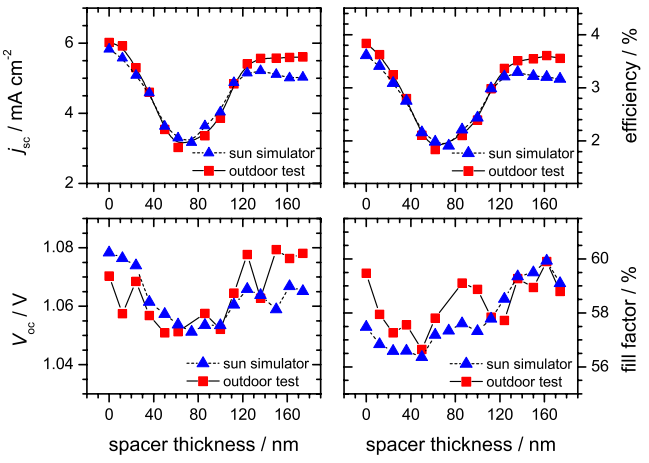

FIG. 4. (Color online) The standard fingerprints (j_{sc}, V_{oc}, FF, η) of the tandem devices as function of the spacer thickness for both illumination with a Steuernagel SC1200 sun simulator (100 mW/cm^2 for a calibrated Si-reference cell) and the real sun during outdoor measurements (1.0 sun).

Author complimentary copy. Redistribution subject to AIP license or copyright, see http://jap.aip.org/jap/copyright.jsp

is expected as function of spacer thickness caused by the interference pattern. This current limiting behavior of the second subcell is confirmed experimentally. In Fig. 4, a period length of about 150 nm is observed. Given that the refractive index of the ZnPc:C_{60} blend is approximately 2, this corresponds to roughly half the mean absorbed wavelength (650 nm). For spacer thicknesses above 150 nm, j_{sc} begins to deviate slightly from the periodic shape and seems to saturate. The variations of V_{oc} in Fig. 4 appear to correlate with the spacer thickness as well, but the relative change is less than 2%. The most likely reason for this are variations in quasi-Fermi level splitting due to variations in charge carrier densities in the second subcell.[32] For single junction organic solar cells, the influence of the charge carrier density on V_{oc} was clearly demonstrated through variations in illumination intensity.[33] The FF mainly reflects the recombination of charge carriers in the active material area as well as the efficiency of charge separation. The small observed fluctuations of FF ($\leqslant 3\%$) show no systematic behavior. In particular, a periodic dependence on the spacer thickness is not observed. An insufficient hole transport in the p-doped spacer layer from the active layer to the recombination contact would lead to a decreasing FF and V_{oc} with increasing thickness, which is not the case.

Consequently, two maxima for η are found: 3.8% for the first and 3.6% for the second maximum (outdoor test) that are mainly determined by j_{sc} variations. These findings verify and considerably expand former results for similar tandem solar cells.[12] There, the spacer was varied for four spacer thicknesses only around the second interference maximum. Thus, the crossover from first to second maximum was not demonstrated. Furthermore, the authors used a thin layer of Au cluster for the recombination contact, resulting in a lower V_{oc} of 0.99 V.

V. COMPARISON OF SIMULATION AND EXPERIMENTS

j_{sc} derived from optical simulations and measurements agree qualitatively and to some extent quantitatively up to 140 nm spacer thickness. In the outdoor measurements (see Fig. 4), j_{sc} of 6.0 mA/cm^2 at 0 nm spacer is measured. The corresponding calculations suggest a j'_{sc} of 6.6 mA/cm^2, suggesting an IQE around 90%. Such high IQE values are possible as reported in literature.[34]

Furthermore, the variations in j'_{sc} of the ITO-sided subcell are observed in the experimental j_{sc} of the tandem device. The minimum predicted by simulation at approximately 75 nm spacer thickness is found at about 70 nm in the experiment. However, in the measurements j_{sc} varies from minimum to maximum by a factor of 2 in the range of spacer variations, in the simulations by a factor of nearly 3. Thus, the device delivers more current than if it had to be equal to the minimum current of either subcell, which is possible[35] and might be further offset by leakage currents.

The qualitative agreement of the simulated and measured shape of j_{sc} as function of the spacer thickness continues up to the second maximum between simulation and experiment. Then quantitative deviations between simulation and experiments grow. The second current maximum is predicted for 170 nm spacer thickness, whereas in experiment the maximum j_{sc} is observed at 140 nm. This discrepancy might have several reasons. The refractive index of all materials depends on the morphology of the layer that can be slightly different in the solar cell stack compared to the thin pristine film from which the n&k values are determined. Furthermore, the used methods and fitting algorithms to determine n&k-values introduce a certain uncertainty despite careful crosschecks. The n&k-values for the 2% doped n-C_{60} layer and the 10% doped p-DiNPB layer in the recombination contact are approximated by the pristine C_{60} and by 5% doped p-DiNPB, respectively. This is a reasonable assumption based on the low doping concentration and the thin layer thickness. Yet, it might have a small influence on the refractive index in the spacer layers. Lastly, although different preparation conditions can be ruled out between the shown devices (all samples are processed in the same run), the absolute thickness of each layers might deviate by 5%–10% depending on the preparation conditions.

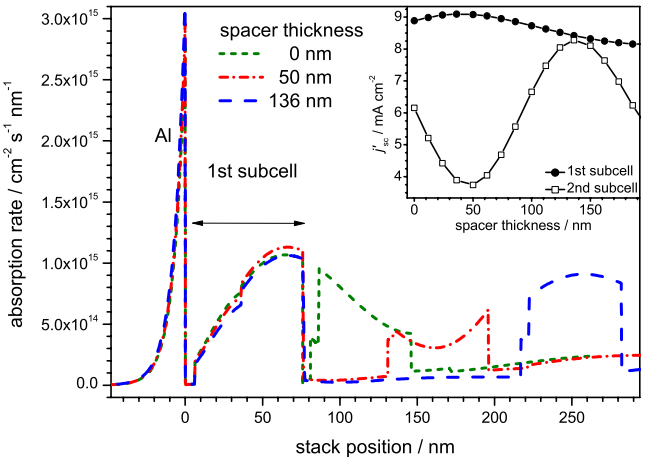

FIG. 5. (Color online) Optical simulations of number n_{ph} of absorbed photons per unit area, time, and propagation length for different spacer thicknesses. The tandem device structure is as before, but has thicker absorbing subcells with 30 nm C_{60}+40 nm ZnPc:C_{60} (1:1) in the first and 60 nm ZnPc:C_{60} (1:1) in the second subcell. Inset: Calculated j'_{sc} for either subcell assuming an IQE of unity.

From the second maximum, the measured j_{sc} begins to deviate from the periodic behavior observed in the simulations. This is probably caused by a limited coherence length of both light sources. If the second subcell is placed far away from the reflecting electrode, i.e., in a distance greater than the coherence length of the illumination light, the absorption in the second subcell is expected to be governed by Beer's law for direct and reflected light and will be independent of the distance, that is, the spacer layer thickness.

In the presented series the layer thicknesses of the absorbers are 55 and 35 nm for the first and second subcells, respectively. Thus, both subcells still fit into the first interference maximum and the maximum j_{sc} and efficiency is reached without spacer layer (see Figs. 2 and 4). However, given the rapid development in small molecules and methods to retain high fill factors in thicker absorbing layers,[36,37] thicker layers will soon be used in small molecule based organic tandem solar cells as well. In Fig. 5, the simulated results of a tandem device is shown, in which the absorbing

Author complimentary copy. Redistribution subject to AIP license or copyright, see http://jap.aip.org/jap/copyright.jsp

layers are increased to 70 and 60 nm for the first and second subcells, respectively. Again, the overall j_{sc} is at all times limited by the second subcell. For 0 nm spacer, the calculated j'_{sc} from the second subcell is 6.1 mA/cm^2, about 0.5 mA/cm^2 less than shown in Fig. 2 for thin absorber layers. Thus, despite the increased absorber layer thickness (the blend layer thickness is more than doubled) the overall current density is smaller. This shows that the thicker subcells do not both fit into the first optical interference maximum anymore and 0 nm is not the optimal spacer value. A spacer thickness of approximately 135 nm is required for j'_{sc} from the second subcell to reach its maximum and current matching at about 8.2 mA/cm^2. Hence, an optical spacer layer between the subcells will become an essential requirement for optimized devices.

VI. CONCLUSION

Tandem solar cells are a promising concept to overcome thermalization losses and sub-band-gap transmission in organic thin film devices. To obtain an optimized device, the currents of both subcells have to match. Besides the material related absorption potential, i.e., the absorption coefficient of the absorbing materials, the thin film optics of the device has to be taken into account. We demonstrate this effect by a systematic thickness variation in a p-doped transparent spacer layer (0 to 186 nm) between two subcells in optical simulations and experiments, which agree qualitatively and to an extent quantitatively up to 140 nm. For the used absorber layers consisting of ZnPc and C_{60} (see Fig. 1), placing both subcells into the first interference maximum with 0 nm spacer is still possible and leads to a maximum in η of 3.8% (outdoor measurement). Increasing the spacer thickness to 70–75 nm the second subcell is placed in the first interference minimum and j_{sc} drops by a factor of 2–3 and so does η. The measured j_{sc} and η recover nearly to their initial value at 140 nm spacing. V_{oc} and FF remain constant within 3%, showing that Ohmic losses are negligible within this spacer range and that placing both subcells into separate interference maxima yields a comparable device performance. This opens the door for thicker absorber layers, which can absorb more light due to an increased thickness, but cannot be fitted in the first interference maximum anymore. Optimizing these devices will hence crucially depend on an optical spacer, because the second subcell has to be placed in the second optical interference maximum.

ACKNOWLEDGMENTS

We thank Patricia Freitag and Michael Thomschke for a careful analysis of the thickness reproducibility at our evaporation chamber. Hendrik Linz is acknowledged for helpful discussion about real sun spectra in the outdoor test and the respective airmass. The German Federal Ministry of Education and Science (BMBF) is acknowledged for funding in the framework of InnoProfile project (03IP602).

[1] W. Shockley and H. J. Queisser, J. Appl. Phys. **32**, 510 (1961).
[2] P. Würfel, *Physik der Solarzellen* (Spektrum Akademischer Verlag, Berlin, 2000).
[3] M. A. Green, Physica E (Amsterdam) **14**, 65 (2002).
[4] T. Ameri, G. Dennler, C. Lungenschmied, and C. J. Brabec, Energy Environ. Sci. **2**, 347 (2009).
[5] B. A. Gregg and M. C. Hanna, J. Appl. Phys. **93**, 3605 (2003).
[6] G. Dennler, M. C. Scharber, T. Ameri, P. Denk, K. Forberich, C. Waldauf, and C. J. Brabec, Adv. Mater. (Weinheim, Ger.) **3**, 579 (2008).
[7] A. Donges, Eur. J. Phys. **19**, 245 (1998).
[8] B. Maennig, J. Drechsel, D. Gebeyehu, P. Simon, F. Kozlowski, A. Werner, F. Li, S. Grundmann, S. Sonntag, M. Koch, Appl. Phys. A: Mater. Sci. Process. **79**, 1 (2004).
[9] M. Hiramoto, M. Suezaki, and M. Yokoyama, Chem. Lett. **3**, 327 (1990).
[10] A. Yakimov and S. R. Forrest, Appl. Phys. Lett. **80**, 1667 (2002).
[11] J. Drechsel, B. Maennig, F. Kozlowski, M. Pfeiffer, K. Leo, and H. Hoppe, Appl. Phys. Lett. **86**, 244102 (2005).
[12] A. Hadipour, B. de Boer, J. Wildeman, F. B. Kooistra, J. C. Hummelen, M. G. R. Turbiez, M. M. Wienk, R. A. J. Janssen, and P. W. M. Blom, Adv. Funct. Mater. **16**, 1897 (2006).
[13] G. Dennler, H.-J. Prall, R. Koeppe, M. Egginger, R. Autengruber, and N. S. Sariciftci, Appl. Phys. Lett. **89**, 073502 (2006).
[14] A. Hadipour, B. de Boer, and P. W. M. Blom, J. Appl. Phys. **102**, 074506 (2007).
[15] D. Cheyns, H. Gommans, M. Odijk, J. Poortmans, and P. Heremans, Sol. Energy Mater. Sol. Cells **91**, 399 (2007).
[16] J. Gilot, M. M. Wienk, and R. A. J. Janssen, Appl. Phys. Lett. **90**, 143512 (2007).
[17] J. Y. Kim, K. Lee, N. E. Coates, D. Moses, T. Q. Nguyen, M. Dante, and A. J. Heeger, Science **317**, 222 (2007).
[18] R. Timmreck, S. Olthof, K. Leo, and M. K. Riede, "Highly doped layers as efficient electron-hole recombination contacts for tandem organic solar cells," J. Appl. Phys. (submitted).
[19] Standard IEC 60904-3, Measurement principles for terrestrial pv solar devices with reference spectral irradiance data, International Electrotechnical Commission, Geneva, Switzerland.
[20] The device area is defined from comparison of current measurement with a 3 mm^2 aperture.
[21] K. Walzer, B. Maennig, M. Pfeiffer, and K. Leo, Chem. Rev. (Washington, D.C.) **107**, 1233 (2007).
[22] R. Franke, B. Maennig, A. Petrich, and M. Pfeiffer, Sol. Energy Mater. Sol. Cells **92**, 732 (2008).
[23] G. Schwartz, T. H. Ke, C. C. Wu, K. Walzer, and K. Leo, Appl. Phys. Lett. **93**, 073304 (2008).
[24] S. Reineke, F. Lindner, G. Schwartz, N. Seidler, K. Walzer, B. Lüssem, and K. Leo, Nature (London) **459**, 234 (2009).
[25] J. Drechsel, A. Petrich, M. Koch, S. Pfützner, R. Meerheim, S. Scholz, J. Drechsel, K. Walzer, M. Pfeiffer, and K. Leo, SID Int. Symp. Digest Tech. Papers **37**, 1692 (2006).
[26] O. Heavens, *Optical Properties of Thin Solid Films* (Dover, New York, 1991).
[27] E. Centurioni, Appl. Opt. **44**, 7532 (2005).
[28] T. Fritz, J. Hahn, and H. Böttcher, Thin Solid Films **170**, 249 (1989).
[29] R. Nitsche, Ph.D. thesis, Technical University Dresden, 2005.
[30] Google earth, version 4.3.
[31] P. Peumans, A. Yakimov, and S. R. Forrest, J. Appl. Phys. **93**, 3693 (2003).
[32] C. Uhrich, D. Wynands, S. Sonntag, B. Maennig, M. Pfeiffer, and K. Leo, J. Appl. Phys. **104**, 043107 (2008).
[33] L. J. A. Koster, V. D. Mihailetchi, R. Ramaker, and P. W. M. Blom, Appl. Phys. Lett. **86**, 123509 (2005).
[34] S. H. Park, A. Roy, S. Beaupre, S. Cho, N. Coates, J. S. Moon, D. Moses, M. Leclerc, K. Lee, and A. J. Heeger, Nat. Photonics **3**, 297 (2009).
[35] A. Hadipour, B. de Boer, and P. Blom, Org. Electron. **9**, 617 (2008).
[36] K. Suemori, T. Miyata, M. Hiramoto, and M. Yokoyama, Jpn. J. Appl. Phys., Part 2 **43**, L1014 (2004).
[37] S. Pfuetzner, J. Meiss, A. Petrich, M. Riede, and K. Leo, Appl. Phys. Lett. **94**, 253303 (2009).

Author complimentary copy. Redistribution subject to AIP license or copyright, see http://jap.aip.org/jap/copyright.jsp